ORGANOMETALLICS

pubs.acs.org/Organometallics Article

Synthesis and Catalytic Reactivity of Cobalt Pincer Nitrosyl Hydride Complexes

Jan Pecak, Sarah Fleissner, Luis F. Veiros, Ernst Pittenauer, Berthold Stöger, and Karl Kirchner*

Cite This: *Organometallics* 2021, 40, 278–285 Read Online

ACCESS | Metrics & More | Article Recommendations | Supporting Information

ABSTRACT: The synthesis, characterization, and catalytic activity of low-spin {CoNO}^{8} pincer complexes of the type [Co(PCP)(NO)(H)] are described. These compounds are obtained either by reacting [Co(PCP)(κ^2-BH_4)] with NO and Et_3N or, alternatively, by reacting $[Co(PCP)(NO)]^+$ with boranes, such as $NH_3{\cdot}BH_3$ in solution. The five-coordinate, diamagnetic Co(III) complex [Co(PCP^{NMe}-*i*Pr)(NO)(H)] was found to be the active species in the hydroboration of alkenes with anti-Markovnikov selectivity. A range of aromatic and aliphatic alkenes were efficiently converted with pinacolborane (HBpin) under mild conditions in good to excellent yield. Mechanistic insight into the catalytic reaction is provided by means of isotope labeling, NMR spectroscopy, and APCI/ESI-MS as well as DFT calculations.

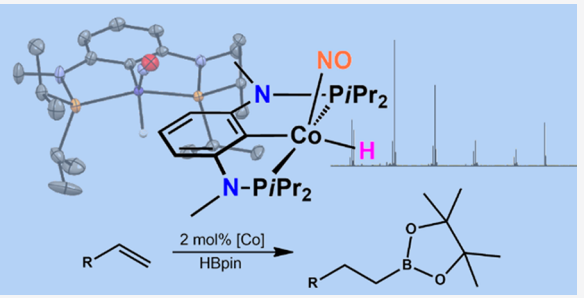

INTRODUCTION

Transition metal hydride complexes play a prominent role in the field of organometallic chemistry. They are often key intermediates in homogeneous catalysis and are important for transformations such as hydrogenations, hydroformylations, or other complex multicomponent reactions.[1,2] PCP and PNP pincer ligands, where phosphane donors are connected via CH_2, O, or NR spacers to an aromatic backbone, proved to be extremely valuable scaffolds for the stabilization and activation of transition metal fragments. Their prominence and popularity are due to the fact that electronic and steric parameters are adjustable and their synthesis often trivial.[3] Over the past two decades, various pincer complexes, primarily based on precious metals, have been utilized in homogeneous catalysis. However, the recent trend and focus lies on the replacement of noble metals with environmentally benign and cheap base metals. In contrast to late transition metals, first-row transition elements can also exhibit different coordination geometries, various spin states, and complicated electronic structures that could alter catalytic pathways or lead to different selectivities in chemical transformations.[4] With respect to 3d transition metals, the chemistry of nickel PCP complexes is quite comprehensive, while studies on iron, cobalt, and manganese PCP pincer complexes remain significantly less common. This may be attributed to the failure of many simple salts to cleave the C_{arene}–H bond in the ligand and to thermodynamic instability of the hydride complexes formed. In recent years, metal catalyzed hydroboration has received considerable attention, since organoboron compounds can be very useful reagents in synthetic organic chemistry.[5] Among others, the group of Chirik provided ground-breaking work in this field and demonstrated the proficiency of selective cobalt catalysts in such transformations.[6] It is noteworthy that complexes with nitrosyl ligands (NO) are relatively unexplored in homogeneous catalysis despite their importance in biological systems. The NO ligand exhibits redox noninnocent properties and can therefore bind in various modes to a metal center, i.e., linear, intermediate, and bent. This ability can be used to generate a vacant coordination site on demand or stabilize intermediates by supplying or detracting electron density.[7] Very recently, our group reported on a set of new {CoNO}^{8} PCP pincer complexes and an initial study on their catalytic reactivity.[8] In this contribution, we describe the synthesis, characterization, and catalytic application of new cobalt {CoNO}^{8} hydride complexes in anti-Markovnikov alkene hydroboration. Two different synthetic approaches, X-ray structures and a DFT-modeled mechanism, are presented.

RESULTS AND DISCUSSION

As reported earlier, nitrosyl complex **1a** was shown to be catalytically active for the reductive hydroboration of aromatic and aliphatic nitriles at ambient temperatures. Moreover, there was strong evidence for a hydride species involved in the catalytic cycle. In the following, two different convergent approaches to such a species will be discussed. The starting materials for the present study, [Co(PCP^{NMe}-*i*Pr)(NO)]BF_4

Received: November 28, 2020
Published: January 5, 2021

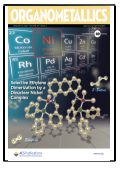

https://dx.doi.org/10.1021/acs.organomet.0c00755
Organometallics 2021, 40, 278–285

(**1a**) and [Co(PCP^{O}-*i*Pr)(NO)]PF_6 (**1b**), were prepared according to recent literature. Inspired by the chemical processes involved in the hydroboration of nitriles, we reacted **1a** with various hydrogen sources such as pinacolborane (HBpin), $NH_3{\cdot}BH_3$, $BH_3{\cdot}THF$, $Ph_2HP{\cdot}BH_3$, or Ph_3SnH in THF and identified the product as a diamagnetic {CoNO}^{8} hydride complex similar to that proposed in a preceding study by Tonzetich and co-workers (Scheme 1).[9] Stoichiometric

Scheme 1. Synthesis of Complexes 2a and 2b

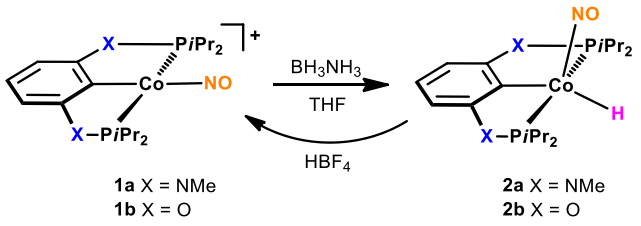

reaction of **1a** or **1b**, respectively, with $NH_3{\cdot}BH_3$ in THF led to formation of the desired hydride pincer complexes **2a** and **2b** in 68 and 58% isolated yield. No reaction was however observed when $Me_2HN{\cdot}BH_3$, $Me_3N{\cdot}BH_3$, or NaH was used instead. Treatment of hydride complex **2a** with HBF_4 in Et_2O resulted in back-formation of cationic **1a**, as confirmed by $^{31}P\{^1H\}$ NMR and ATR-IR spectroscopy.

The new species was fully characterized by a combination of ^1H, $^{13}C\{^1H\}$, and $^{31}P\{^1H\}$ NMR spectroscopy, ATR-IR spectroscopy, and HR-MS analysis. The proton decoupled ^{31}P spectrum of **2a** exhibits a broad resonance at 175 ppm and displays a triplet resonance at −9.23 ppm (J_{HP} = 57 Hz) in the proton NMR spectrum, consistent with a cobalt hydride. Moreover, one strong absorption band for the characteristic NO stretching mode is detected at 1660 cm^{-1} in the IR spectrum and a weak band at 1847 cm^{-1} attributable to the Co−H vibrational mode. In order to unequivocally establish the ligand arrangement around the metal center, the solid-state structure of **2a** was determined by X-ray diffraction. Suitable single crystals were grown from a saturated pentane solution kept at −20 °C. A view of the molecular structure is depicted in Figure 1 with selected bond distances and angles reported in captions. The complex adopts a distorted square pyramidal geometry (τ_5 < 0.2)[10] with the metal center surrounded by three donor atoms of the PCP ligand and the NO group

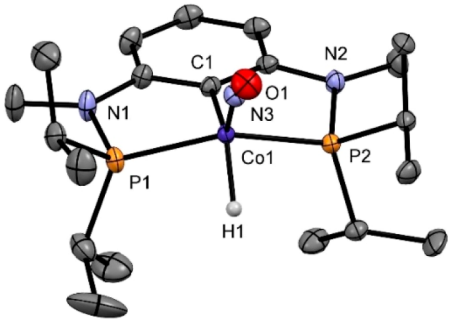

Figure 1. Structural view of **2a** showing 50% displacement ellipsoids (Z' = 5, H atoms except for H1A omitted for clarity). Selected bond lengths (Å) and angles (deg): Co1−C1 1.988(2), Co1−H1 1.45(4), Co1−P1 2.1690(7), Co1−P2 2.1543(7), Co1−N3 1.659(2), N3−O1 1.183(3), P2−Co1−P1 145.64(3), C1−Co1−H1 130.1(16), Co1−N3−O1 163.9(2).

occupying the apical position. The mean N−O bond distance is 1.182(3) Å, and the Co−N−O angle of 165.5(2)° is in the range expected for an intermediate to bent configuration. The hydride atom itself could be located in the difference Fourier maps. The mean Co−H distance was refined to 1.39(5) Å. A direct structural comparison can be drawn to isoelectronic [Co(PNP-*t*Bu)(NO)(H)] that was reported recently by Krishnan et al. to have a Co−N−O angle of 151.7(5)° and a N−O bond distance of 1.195(7) Å.[9]

It is worth mentioning that penta-coordinate {MNO}^{8} complexes naturally tend to show bent M−N−O arrangements when adopting a square-pyramidal geometry and a rather linear arrangement in cases with a trigonal-bipyramidal geometry.[11,12] Moreover, Berke and Burger concluded from a comprehensive experimental and theoretical survey that the NO ligand leads to a strong polarization of the M−H bond and that the reactivity toward alkyne insertion and carbonyl reduction chemistry is enhanced.[13] A selection of other nitrosyl hydride complexes can be found in further literature.[14]

Similarly, low-spin complex **2b** exhibits a broad resonance at 231 ppm in the $^{31}P\{^1H\}$ NMR spectrum and a strong NO band at 1693 cm^{-1} in the ATR-IR spectrum. Regarding the electronic structure, the metal center in the {CoNO}^{8} species **2a** and **2b** is better described as Co(III) rather than Co(II). Although the increased Co−N−O angle and stronger distorted geometry as compared to [Co^{III}(PCP^{NMe}-*i*Pr)(NO)Cl] (cf. Co−N−O 140.1°) could suggest a different electronic behavior, no evidence was found to support a Co(II) character.[8] An unequivocal assignment is hindered by orbital mixing, but the *d*-splitting calculated for complex **2a** indicates a d^6 species (see Figure 2) and, thus, a Co(III) metal center. Moreover, a clear negative charge on the NO ligand, C_{NO} =

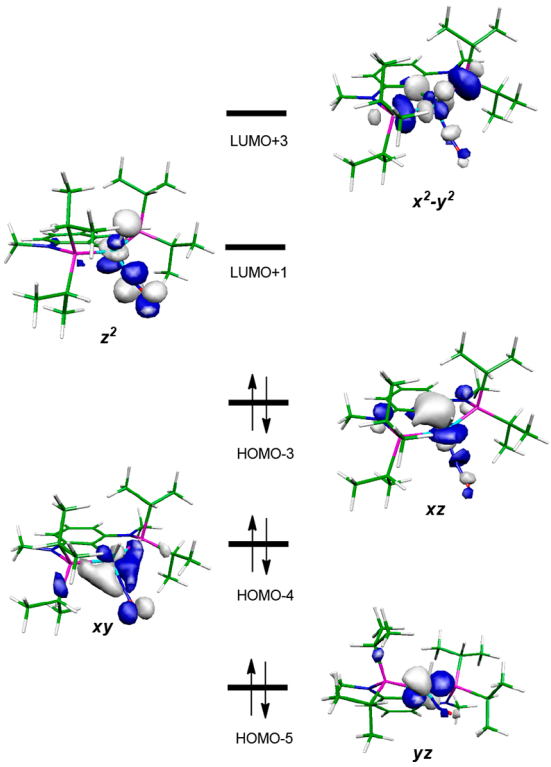

Figure 2. *d*-Splitting of [Co(PCP^{NMe}-*i*Pr)(NO)(H)] calculated by DFT (PBE0/6-31G**).

https://dx.doi.org/10.1021/acs.organomet.0c00755
Organometallics 2021, 40, 278−285

−0.24, calculated by a NPA analysis (see Computational Details) as well as a Co−N_{NO} Wiberg index typical of a single bong (WI = 0.96) strongly support the same conclusion.

An alternative synthetic protocol to obtain these hydride complexes was successfully applied starting from the related borohydride species **3a** and **3b**. Reaction of the paramagnetic (S = 1/2) borohydride complex [Co(PCP^{NMe}-*i*Pr)(κ^2-BH_4)] (**3a**)[15] with nitric oxide and an excess of Et_3N in benzene led to a color change from pink to deep purple and to the appearance of resonances in the negative region of the ^{1}H NMR spectrum. After extraction and careful workup, **2a** was isolated in 17% yield. In a similar fashion, [Co(PCP^{O}-*i*Pr)(NO)(H)] (**2b**) was obtained in 12% yield starting from the related borohydride species **3b** (Scheme 2).

Scheme 2. Alternative Synthesis of Complexes 3a and 3b

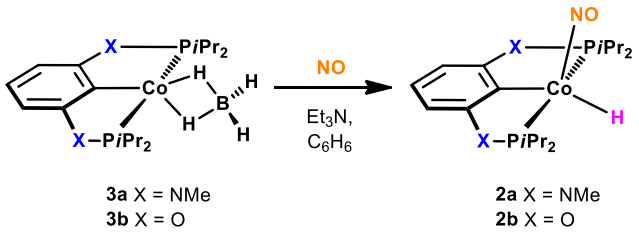

3a X = NMe
3b X = O

2a X = NMe
2b X = O

Starting material **3b** was prepared according to the literature by reacting [Co(PCP^{O}-*i*Pr)Cl] (**4**) with an excess of $NaBH_4$ in THF/EtOH. Complex **3b** was successfully crystallized from a saturated pentane solution at −20 °C and its structure determined by single crystal X-ray diffraction. A structural view is depicted in Figure 3 with selected bond distances and angles reported in captions. The molecular structure and metrics are in accordance with earlier reported borohydride complexes.[15,16]

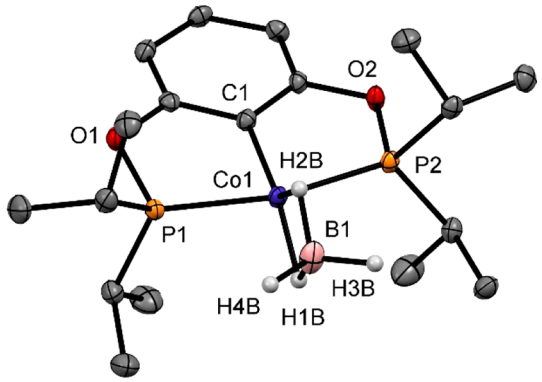

Figure 3. Structural view of **3b** showing 50% displacement ellipsoids (H atoms except for B−H omitted for clarity). Selected bond lengths (Å) and angles (deg): Co1−C1 1.923(2), Co1−B1 2.140(3), Co1−P1 2.1797(7), Co1−P2 2.1744(7), C1−Co1−B1 164.80(11), P1−Co1−P2 162.13(3).

The demonstrated ability of **1a** to hydroborate nitriles prompted us to explore the hydroboration of aromatic and aliphatic alkenes. Initial experiments focused on the hydroboration of 4-fluorostyrene with pinacolborane (HBpin) in the presence of 2 mol % of complex **1a** at 25 °C for a reaction time of 24 h using dry benzene or THF as solvent. In each experiment, a diagnostic color change from colorless to purple was observed after addition of HBpin, indicating the formation of the active catalyst. It needs to be mentioned that the cationic precatalyst itself is insoluble in benzene but formed **2a** quickly enters the liquid phase and causes the color change. Consequently, pure hydride complex **2a** can be used directly for all catalytic transformations without having any impact on the outcome. Moreover, increasing the temperature from room temperature to 40 °C resulted in full conversion of the test substrate within 3 h. For comparison, also complex **1b** was used as precatalyst with 4-fluorostyrene and other substrates (room temperature, 24 h) to show similar results and yields.

Based on these results, we investigated the scope and limitations of complex **1a** using various substrates (Table 1). All catalytic experiments were conducted in the presence of 2 mol % of **1a** in benzene at 25 °C and 24 h without any additives. The precatalyst was favored over direct use of the hydride species due to its air-stability and ease to handle

Table 1. Hydroboration of Alkenes with Precatalyst 1a

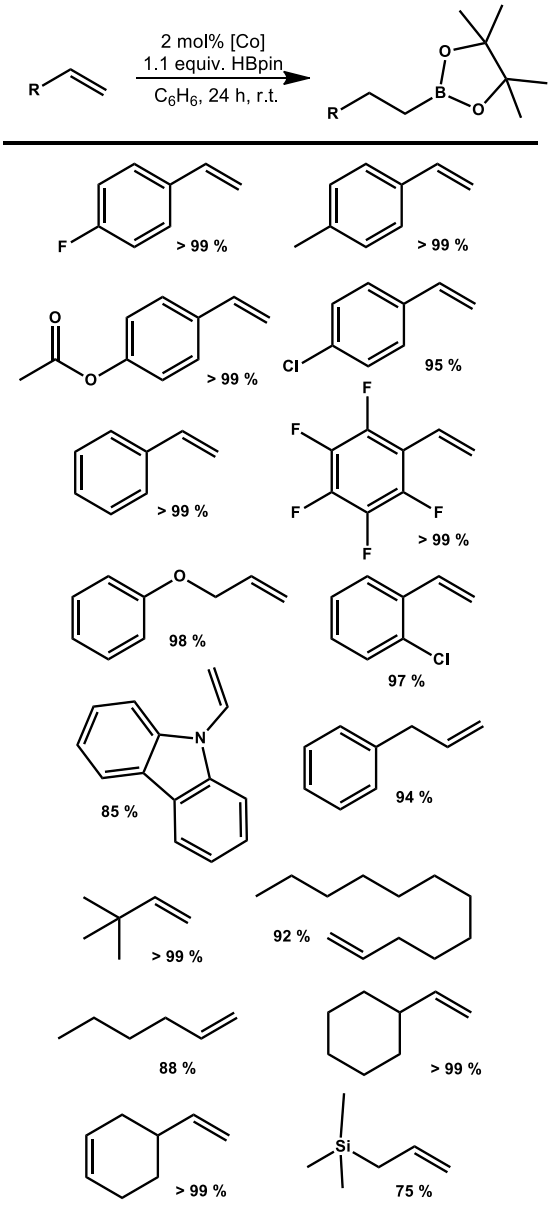

[a]Reaction conditions: 2 mol % of **1a** and 0.3 mmol of substrate in 1 mL of benzene. [b]Conversion rates based on GC-MS measurements.

https://dx.doi.org/10.1021/acs.organomet.0c00755
Organometallics 2021, 40, 278−285

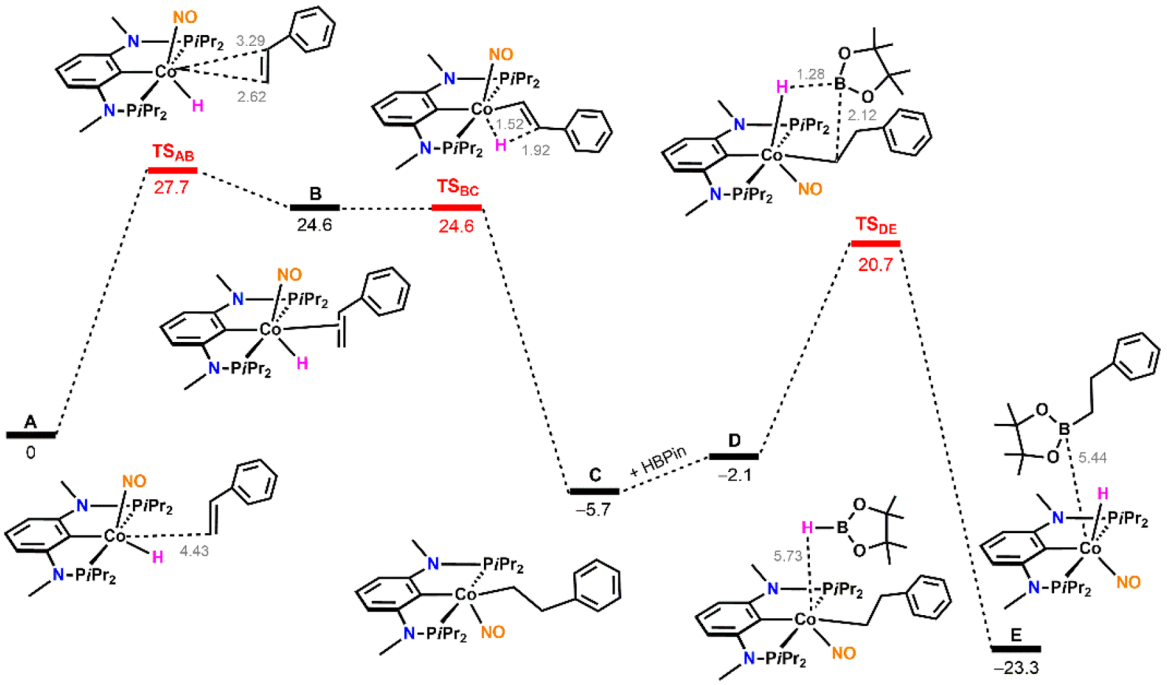

Figure 4. Free energy profile calculated (PBE0-D3/6-31G**) for the hydroboration of styrene with HBpin catalyzed by active species **2a**. The free energy values (kcal/mol) are referenced to the initial reactants, and relevant distances (Å) are indicated in gray color.

without a glovebox. The best results could be obtained for aromatic alkenes bearing both electron-withdrawing and -donating substituents with linear to branched ratios of 98:2 or higher and yields >95%. The hydroboration of 4-vinylcyclohexene, a substrate bearing an internal double bond, proceeded selectively at the terminal alkene position. Ester functions were not affected or reduced. Transformations of sterically more hindered substrates and aliphatic alkenes performed well with 3−5% fully hydrogenated products and yields >85%. One notable exception is allyltrimethylsilane which was converted with 75% yield with a linear to branched ratio of 85:15.

DFT calculations were carried out to establish a reasonable mechanism for the hydroboration of styrene with hydride complex **2a** as the initial active species. The free energy profile is shown in Figure 4. In the first step of the calculated mechanism, olefin coordination takes place forming the π-adduct **B**. The initial barrier of 27.7 kcal/mol seems rather high and may be slightly overestimated, but it could explain the long reaction time for full conversion. It is worth noting how the NO group is electronically involved in the catalytic cycle: Starting from the free hydride complex with a calculated Co−N−O angle of 159° (exp. 165.5°), strong bending occurs toward a value of 122° when **B** is reached. That bending is associated with charge transfer to NO, that has a charge of C = −0.35 in **B**, compared with C = −0.24 in complex **2a**, showing the "noninnocent" character of the ligand. The olefin complex is a high-energy intermediate that transforms with no barrier to the alkyl intermediate **C** via insertion into the Co−H bond. In the next steps, HBpin approaches the alkyl intermediate (**D**) and regenerates the hydride complex while a B−C bond is formed. This step is associated with a barrier of 20.7 kcal/mol and eventually leads to the final products. Closing the cycle, from **E** back to **A**, with release of product and addition of a new styrene molecule is an almost thermoneutral process, with ΔG = −0.2 kcal/mol.

The reaction mechanism was probed using deuterium labeling experiments and spectroscopic methodology (see the Supporting Information).

Using benzene-d_6 as solvent allowed for a continuous monitoring of the reaction showing the prevalence of the hydride species for hours until quenching to air. When the hydroboration of styrene-d_8 with HBpin was performed in benzene-d_6, the anti-Markovnikov product was formed exclusively with the hydrogen atom being in the benzylic position. Moreover, addition of Hg did not affect the overall conversion or selectivity. High-resolution mixed mode ESI-/APCI mass spectrometry[17] was then used to detect possible catalytic intermediates: With 1-hexene as a test substrate instead of styrene, the proposed insertion product [Co(PCP^{NMe}-iPr)(NO)(C$_6$H$_{13}$)] (*vide supra*, intermediate **C**) was successfully detected as [M−H]$^+$ with m/z 540.2679 in THF solution (see Figure 5). All findings support the proposed mechanism.

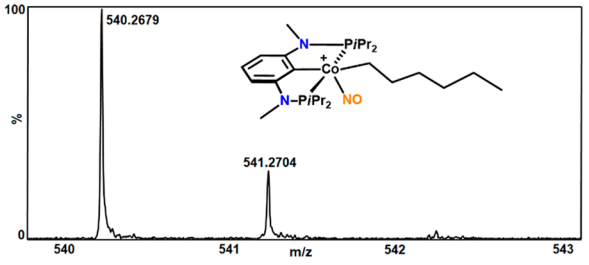

Figure 5. Mixed mode APCI-ESI mass spectrum ([M−H]$^+$) of the intermediate formed in THF after hexene insertion into **2a** during a catalysis experiment. The MS spectrum was measured after 1 h using the direct infusion technique.

https://dx.doi.org/10.1021/acs.organomet.0c00755
Organometallics 2021, 40, 278−285

CONCLUSION

We reported on the synthesis of two novel {CoNO}^{8} nitrosyl hydride complexes of the type [Co(PCP)(NO)(H)] supported by PCP pincer ligands that are connected via NMe/O spacers to an aromatic backbone. There are two synthetic approaches to obtain these compounds: one using a borohydride precursor and an alternative, more efficient one starting from [Co(PCP)(NO)]$^+$. All compounds were fully characterized by means of NMR and IR spectroscopy, HR-MS, and single crystal XRD. It was shown that cationic **1a** can be used as a precatalyst for the efficient hydroboration of aromatic and aliphatic alkenes. We presented detailed mechanistic investigations proving that the hydride complex is an active species and showing that insertion products can be trapped by means of high-resolution mass spectrometry. Furthermore, DFT calculations were used to support the experimental findings and explain the effect of the electronically "non-innocent" NO group.

EXPERIMENTAL SECTION

General Information. All manipulations were performed under an inert atmosphere of argon by using Schlenk techniques or in an MBraun inert-gas glovebox. The solvents were purified according to standard procedures.[18] The deuterated solvents were purchased from Aldrich and dried over 4 Å molecular sieves. Nitric oxide (NO 2.5) was purchased from MESSER GmbH (Gumpoldskirchen, Austria). The synthesis of the complexes, [Co(PCP^{NMe}-*i*Pr)(NO)]BF_4 (**1a**), [Co(PCP^{O}-*i*Pr)(NO)]PF_6 (**1b**), [Co(PCP^{NMe}-*i*Pr)(κ^2-BH_4)] (**3a**), and [Co(PCP^{O}-*i*Pr)Cl] (**4**), was carried out according to the literature.[8,15] All ^{1}H, ^{13}C{^{1}H}, and ^{31}P{^{1}H} NMR spectra were recorded on Bruker AVANCE-250 and AVANCE-400 spectrometers. ^{1}H and ^{13}C{^{1}H} NMR spectra were referenced internally to residual protio-solvent and solvent resonances, respectively, and are reported relative to tetramethylsilane (δ = 0 ppm). ^{31}P{^{1}H} NMR spectra were referenced externally to H_3PO_4 (85%) (δ = 0 ppm). Infrared spectra were recorded in attenuated total reflection (ATR) mode on a PerkinElmer Spectrum Two FT-IR spectrometer.

Synthesis. [Co(PCP^{NMe}-*i*Pr)(NO)(H)] (2a). Method A. Nitric oxide (4 mL, 1 atm) was injected into the headspace of a solution of [Co(PCP^{NMe}-*i*Pr)(κ^2-BH_4)] (30 mg, 0.06 mmol) and Et_3N (30 μL) in benzene (2 mL). After an immediate color change to purple, all volatiles were removed under reduced pressure. The remaining dark colored solid was extracted into pentane and the extract filtered through a syringe filter. The solvent was removed to obtain a purple solid. Yield: 4 mg (15%). **Method B.** To a solution of NH_3BH_3 (2.3 mg, 0.07 mmol) in THF (3 mL) was added solid [Co(PCP^{NMe}-*i*Pr)(NO)]BF_4 (40 mg, 0.07 mmol). The reaction mixture was stirred for 5 min at room temperature, and then, all volatiles were removed under reduced pressure. The remaining brownish green solid was extracted into pentane and the extract filtered through a syringe filter. The solvent was partially removed in a vacuum and the solution put in a freezer at −20 °C to yield a dark purple crystalline solid. Yield: 23 mg (68%). ^{1}H NMR (250 MHz, δ, C_6D_6): 7.27 (t, J = 7.8 Hz, 1H, ph), 6.21 (d, J = 7.8 Hz, 2H, ph), 2.62 (s, 6H, CH_3), 2.27 (m, 3H, CH_3), 1.74 (m, 3H, CH_3), 1.36 (app. q., J = 7.6 Hz, 6H, CH_3), 1.17 (app. q., J = 7.6 Hz, 6H, CH_3), 0.92 (app. q., J = 7.6 Hz, 6H, CH_3), 0.52 (app. q., J = 7.6 Hz, 6H, CH_3), −9.24 (t, J = 59.6 Hz, 1H, H). ^{13}C{^{1}H} NMR (151 MHz, δ, C_6D_6): 151.6 (t, J = 14.7 Hz), 125.8, 99.1, 30.8 (t, J = 8.6 Hz), 30.4 (t, J = 3.0 Hz), 29.3, 28.0 (t, J = 15.7 Hz), 17.8 (t, J = 2.7 Hz), 17.5 (m), 17.06. ^{31}P{^{1}H} NMR (101 MHz, δ, C_6D_6): 175.0. IR (ATR, cm^{-1}): 1660 (ν_{NO}), 1847 (ν_{CoH}). HR-MS (ESI$^+$, MeOH): m/z calcd for $C_{20}H_{38}CoNO_3P_2$ [M]$^+$ 457.1822, found 457.1825.

[Co(PCP^{O}-*i*Pr)(NO)(H)] (2b). Method A. The synthesis was performed in a similar fashion to **3a** with [Co(PCP^{O}-*i*Pr)(BH_4)] (30 mg, 0.07 mmol), Et_3N (30 μL), and NO (4 mL, 1 atm) in benzene (2 mL). Yield: 6 mg (21%). **Method B.** The synthesis was performed in a similar fashion to **3a** with [Co(PCP^{NMe}-*i*Pr)(NO)]PF_6 (40 mg, 0.07 mmol) and NH_3BH_3 (2.1 mg, 0.07 mmol) in THF (3 mL). Yield: 17 mg (58%). ^{1}H NMR (400 MHz, δ, C_6D_6): 6.90 (t, J = 7.8 Hz, 1H, ph), 6.78 (d, J = 7.8 Hz, 2H, ph), 2.56−2.43 (m, 2H, CH), 1.91−1.79 (m, 2H, CH), 1.31 (app. q., J = 7.0 Hz, 6H, CH_3), 1.23 (app. q., J = 6.0 Hz, 6H, CH_3), 0.90 (app. q., J = 7.0 Hz, 6H, CH_3), 0.78 (app. q., J = 7.3 Hz, 6H, CH_3), −9.75 (t, J = 58.3 Hz, 1H, H). ^{13}C{^{1}H} NMR (101 MHz, δ, C_6D_6): 165.1, 104.6, 32.0 (t, J = 10.8 Hz), 30.6 (t, J = 13.9 Hz), 30.1, 29.8, 17.2 (t, J = 3.5 Hz), 17.1, 16.9, 1.0. ^{31}P{^{1}H} NMR (162 MHz, δ, C_6D_6): 231.8. IR (ATR, cm^{-1}): 1693 (ν_{NO}), 1831 (ν_{CoH}). HR-MS (ESI$^+$, THF): m/z calcd for $C_{18}H_{31}CoNO_3P_2$ [M−H]$^+$ 430.1110, found 430.1102.

[Co(PCP^{O}-*i*Pr)(κ^2-BH_4)] (3b). To a solution of [Co(PCP^{O}-*i*Pr)Cl] (100 mg, 0.23 mmol) in a 1:1 mixture of THF and EtOH (3 mL) was added $NaBH_4$ (18 mg, 0.45 mmol). The reaction mixture was stirred for 3 h at room temperature, and the solvent was removed under reduced pressure. The solid was extracted into pentane (15 mL) and the solution filtered through a syringe filter. The solvent was partially removed in a vacuum and the solution put in a freezer at −20 °C to yield a dark yellow crystalline solid. Yield: 72 mg (76%). IR (ATR, cm^{-1}): 2300 (ν_{BH}), 2374 (ν_{BH}). Anal. Calcd for $C_{18}H_{35}CoBO_2P_2$ (415.16): C, 52.07; H, 8.50. Found: C, 51.92; H, 7.92.

General Procedure for the Hydroboration of Alkenes. The alkene substrate (0.30 mmol, 1 equiv), nitrosyl complex **1a** (2 mol %), and pinacolborane (HBpin, 1.1 equiv) were mixed with 1 mL of anhydrous benzene (or THF) in a glass vial and stirred at room temperature for 24 h. After completion of the reaction, it was quenched by exposure to air and the crude reaction mixture was analyzed by gas chromatography (GC-MS). The reaction mixture was then added to 0.1 mL of water, extracted with 3 mL of petrol ether, and the extract filtered through a plug of silica. After evaporating all volatiles under reduced pressure, the obtained compounds where characterized by ^{1}H and ^{13}C{^{1}H} NMR spectroscopy.

Mass Spectrometry. High-resolution accurate mass spectra were recorded on an Agilent 6545 QTOF equipped with an Agilent MMI ion source (Agilent Technologies, Santa Clara, CA, USA) which can be operated in mixed ESI and APCI mode. Measured accurate mass data for confirming calculated elemental compositions were typically within ±3 ppm accuracy. The mass calibration was performed with a commercial mixture of perfluorinated trialkyl-triazines (ES Tuning Mix, Agilent Technologies, Santa Clara, CA, USA). In all experiments, a direct infusion technique was used and samples were prepared in a glovebox.

X-ray Structure Determination. X-ray diffraction data for **1b** and **2a** (2044562 and 2044563) were collected at T = 100 K in a dry stream of nitrogen on a Bruker Kappa APEX II diffractometer system using graphite-monochromatized Mo Kα radiation (λ = 0.71073 Å) and fine sliced ϕ- and ω-scans. Data were reduced to intensity values with SAINT, and an absorption correction was applied with the multiscan approach implemented in SADABS.[19] The structures were solved by the dual space method implemented in SHELXT[20] and refined against F^2 with SHELXL.[21] Non-hydrogen atoms were refined with anisotropic displacement parameters. The H atoms attached to C were placed in calculated positions and thereafter refined as riding on the parent atoms. The hydride H atoms were located in difference Fourier maps and freely refined. Molecular graphics were generated with MERCURY.[22]

Computational Details. The computational results presented have been achieved in part using the Vienna Scientific Cluster (VSC). All calculations were performed using the Gaussian 09 software package[23] without symmetry constraints. The optimized geometries were obtained with the PBE0 functional. That functional uses a hybrid generalized gradient approximation (GGA), including a 25% mixture of Hartree−Fock[24] exchange with DFT[25] exchange correlation, given by the Perdew, Burke, and Ernzerhof functional (PBE).[26] The basis set used consisted of the Stuttgart/Dresden ECP (SDD) basis set[27] to describe the electrons of cobalt and a standard 6-31G(d,p) basis set[28] for all other atoms. Transition state optimizations were performed with the synchronous transit-guided quasi-Newton method (STQN) developed by Schlegel et al.,[29] following extensive searches of the

https://dx.doi.org/10.1021/acs.organomet.0c00755
Organometallics 2021, 40, 278−285

potential energy surface. Frequency calculations were performed to confirm the nature of the stationary points, yielding one imaginary frequency for the transition states and none for the minima. Each transition state was further confirmed by following its vibrational mode downhill on both sides and obtaining the minima presented on the energy profiles. The electronic energies were converted to free energy at 298.15 K and 1 atm by using zero-point energy and thermal energy corrections based on structural and vibration frequency data calculated at the same level. The free energy values presented were corrected for dispersion by means of the Grimme DFT-D3 method[30] with Becke and Johnson short distance damping.[31] The NPA analysis[32] was performed with the NBO 5.0 program,[33] and the orbital representations were obtained with Molekel.[34]

■ ASSOCIATED CONTENT

Supporting Information

The Supporting Information is available free of charge at https://pubs.acs.org/doi/10.1021/acs.organomet.0c00755.

^{1}H, $^{13}C\{^{1}H\}$, and $^{31}P\{^{1}H\}$ NMR spectra of all complexes and organic products (PDF)

Optimized Cartesian coordinates for DFT-calculated structures (XYZ)

Accession Codes

CCDC 2044562−2044563 contain the supplementary crystallographic data for this paper. These data can be obtained free of charge via www.ccdc.cam.ac.uk/data_request/cif, or by emailing data_request@ccdc.cam.ac.uk, or by contacting The Cambridge Crystallographic Data Centre, 12 Union Road, Cambridge CB2 1EZ, UK; fax: +44 1223 336033.

■ AUTHOR INFORMATION

Corresponding Author

Karl Kirchner − *Institute of Applied Synthetic Chemistry, Vienna University of Technology, A-1060 Vienna, Austria;* orcid.org/0000-0003-0872-6159; Email: karl.kirchner@tuwien.ac.at

Authors

Jan Pecak − *Institute of Applied Synthetic Chemistry, Vienna University of Technology, A-1060 Vienna, Austria*

Sarah Fleissner − *Institute of Applied Synthetic Chemistry, Vienna University of Technology, A-1060 Vienna, Austria*

Luis F. Veiros − *Centro de Química Estrutural and Departamento de Engenharia Química, Instituto Superior Técnico, Universidade de Lisboa, 1049-001 Lisboa, Portugal;* orcid.org/0000-0001-5841-3519

Ernst Pittenauer − *Institute of Chemical Technologies and Analytics, Vienna University of Technology, A-1060 Vienna, Austria*

Berthold Stöger − *X-Ray Center, Vienna University of Technology, A-1060 Vienna, Austria;* orcid.org/0000-0002-0087-474X

Complete contact information is available at: https://pubs.acs.org/10.1021/acs.organomet.0c00755

Notes

The authors declare no competing financial interest.

■ ACKNOWLEDGMENTS

Financial support by the Austrian Science Fund (FWF) is gratefully acknowledged (Project No. P 33016-N). Centro de Química Estrutural acknowledges the financial support of Fundação para a Ciência e Tecnologia (UIDB/00100/2020).

■ REFERENCES

(1) For reviews on transition metal hydrides, see: (a) Kaesz, H. D.; Saillant, R. B. Hydride complexes of the transition metals. *Chem. Rev.* **1972**, *72*, 231−281. (b) Pearson, R. G. The transition-metal-hydrogen bond. *Chem. Rev.* **1985**, *85*, 41−49. (c) Eberhardt, N. A.; Guan, H. Nickel Hydride Complexes. *Chem. Rev.* **2016**, *116*, 8373−8426. (d) Hoskin, A. J.; Stephan, D. W. Early transition metal hydride complexes: synthesis and reactivity. *Coord. Chem. Rev.* **2002**, *233−234*, 107−129. (e) Heinekey, D. M.; Oldham, W. J. Coordination Chemistry of Dihydrogen. *Chem. Rev.* **1993**, *93*, 913−926. (f) McGrady, G. S.; Guilera, G. The multifarious world of transition metal hydrides. *Chem. Soc. Rev.* **2003**, *32*, 383−392.

(2) Selected examples: (a) Tanaka, R.; Yamashita, M.; Nozaki, K. Catalytic Hydrogenation of Carbono Dioxide Using Ir(III)-Pincer Complexes. *J. Am. Chem. Soc.* **2009**, *131*, 14168−14169. (b) Langer, R.; Leitus, G.; Ben-David, Y.; Milstein, D. Efficient Hydrogenation of Ketones Catalyzed by an Iron Pincer Complex. *Angew. Chem., Int. Ed.* **2011**, *50*, 2120−2124. (c) Nielsen, M.; Kammer, A.; Cozzula, D.; Junge, H.; Gladiali, S.; Beller, M. Efficient Hydrogen Production from Alcohols under Mild Reaction Conditions. *Angew. Chem.* **2011**, *123*, 9767−9771. (d) Breitenfeld, J.; Scopelliti, R.; Hu, X. Synthesis, Reactivity, and Catalytic Application of a Nickel Pincer Hydride Complex. *Organometallics* **2012**, *31*, 2128−2136. (e) Guard, L. M.; Hebden, T. J.; Linn, D. E.; Heinekey, D. M. Pincer-Supported Carbonyl Complexes of Cobalt(I). *Organometallics* **2017**, *36*, 3104−3109. (f) Gorgas, N.; Alves, L. G.; Stöger, B.; Martins, A. M.; Veiros, L. F.; Kirchner, K. Stable, Yet Highly Reactive Nonclassical Iron(II) Polyhydride Pincer Complexes: Z-Selective Dimerization and Hydroboration of Terminal Alkynes. *J. Am. Chem. Soc.* **2017**, *139*, 8130−8133. (g) Larionov, E.; Li, H.; Mazet, C. Well-defined transition metal hydrides in catalytic isomerizations. *Chem. Commun.* **2014**, *50*, 9816−9826. (h) Merz, L. S.; Blasius, C. K.; Wadepohl, H.; Gade, L. H. Square Planar Cobalt(II) Hydride versus T-Shaped Cobalt(I): Structural Characterization and Dihydrogen Activation with PNP-Cobalt Pincer Complexes. *Inorg. Chem.* **2019**, *58*, 6102−6113.

(3) For reviews on pincer complexes, see: (a) Gossage, R. A.; van de Kuil, L. A.; van Koten, G. Diaminoarylnickel(II) "pincer" complexes: mechanistic consideration in the Kharasch addition reaction, controlled polymerization, and dendrimeric transition metal catalysis. *Acc. Chem. Res.* **1998**, *31*, 423−431. (b) Albrecht, M.; van Koten, G. Platinum group organometallics based on "Pincer" complexes: sensors, switches, and catalysts in memory of Prof. Dr. Luigi M. Venanzi and his pioneering work in organometallic chemistry, particularly in PCP pincer chemistry. *Angew. Chem., Int. Ed.* **2001**, *40*, 3750−3781. (c) van der Boom, M. E.; Milstein, D. Cyclometalated phosphine-based pincer complexes: mechanistic insight in catalysis, coordination, and bond activation. *Chem. Rev.* **2003**, *103*, 1759−1792. (d) Singleton, J. T. The uses of pincer complexes inorganic synthesis. *Tetrahedron* **2003**, *59*, 1837−1857. (e) Liang, L. C. Metal complexes of chelating diarylamido phosphine ligands. *Coord. Chem. Rev.* **2006**, *250*, 1152−1177. (f) The Chemistry of Pincer Compounds; Morales-Morales, D., Jensen, C. M., Eds.; Elsevier: Amsterdam, The Netherlands, 2007. (g) Nishiyama, H. Synthesis and use of bisoxazolinyl-phenyl pincers. *Chem. Soc. Rev.* **2007**, *36*, 1133−1141. (h) Benito-Garagorri, D.; Kirchner, K. Modularly Designed Transition Metal PNP and PCP Pincer Complexes Based on Aminophosphines: Synthesis and Catalytic Applications. *Acc. Chem. Res.* **2008**, *41*, 201−213. (i) Choi, J.; MacArthur, A. H. R.; Brookhart, M.; Goldman, A. S. Dehydrogenation and Related Reactions Catalyzed by Iridium Pincer Complexes. *Chem. Rev.* **2011**, *111*, 1761−1779. (j) Selander, N.; Szabo, K. J. Catalysis by Palladium Pincer Complexes. *Chem. Rev.* **2011**, *111*, 2048−2076. (k) Bhattacharya, P.; Guan, H. Synthesis and Catalytic Applications of Iron Pincer Complexes. *Comments Inorg. Chem.* **2011**, *32*, 88−112. (l) Schneider, S.; Meiners, J.; Askevold, B. Cooperative Aliphatic PNP Amido Pincer Ligands - Versatile Building Blocks for Coordination Chemistry and Catalysis. *Eur. J. Inorg. Chem.* **2012**, *2012*, 412−429. (m) *Organo-metallic Pincer Chemistry*; van Koten, G., Milstein, D., Eds.; Springer: Berlin, 2013; Topics in Organometallic

Chemistry Vol. 40. (n) Szabo, K. J.; Wendt, O. F. *Pincer and Pincer-Type Complexes: Applications in Organic Synthesis and Catalysis*; Wiley-VCH: Weinheim, Germany, 2014. (o) Asay, M.; Morales-Morales, D. Non-symmetric pincer ligands: complexes and applications in catalysis. *Dalton Trans.* **2015**, *44*, 17432−17447. (p) Murugesan, S.; Kirchner, K. Non-precious metal complexes with an anionic PCP pincer architecture. *Dalton Trans* **2016**, *45*, 416−439. (q) Valdes, H.; Garcia-Eleno, M. A.; Canseco-Gonzalez, D.; Morales-Morales, D. Recent Advances in Catalysis with Transition-Metal Pincer Compounds. *ChemCatChem* **2018**, *10*, 3136−3172. (r) Valdes, H.; Rufino-Felipe, E.; van Koten, G.; Morales-Morales, D. Hybrid POCZP Aryl Pincer Metal Complexes and their Catalytic Applications. *Eur. J. Inorg. Chem.* **2020**, *2020*, 4418−4424.

(4) Catalysis without Precious Metals; Bullock, R. M., Ed.; Wiley-VCH: Weinheim, Germany, 2010.

(5) (a) Obligacion, J. V.; Chirik, P. J. Earth-abundant transition metal catalysts for alkene hydrosilylation and hydroboration. *Nat. Rev. Chem.* **2018**, *2*, 15−34. (b) Zhang, L.; Zuo, Z.; Wan, X.; Huang, Z. Cobalt-Catalyzed Enantioselective Hydroboration of 1,1-Disubstituted Aryl Alkenes. *J. Am. Chem. Soc.* **2014**, *136*, 15501−15504. (c) Peng, J.; Docherty, J. H.; Dominey, A. P.; Thomas, S. P. Cobalt-catalysed Markovnikov selective hydroboration of vinylarenes. *Chem. Commun.* **2017**, *53*, 4726−4729. (d) Espinosa, M. R.; Charboneau, D. J.; Garcia de Oliveira, A.; Hazari, N. Controlling Selectivity in the Hydroboration of Carbon Dioxide to the Formic Acid, Formaldehyde, and Methanol Oxidation Levels. *ACS Catal.* **2019**, *9*, 301−314. (e) Xi, T.; Lu, Z. Cobalt-Catalyzed Ligand-Controlled Regioselective Hydroboration/Cyclization of 1,6-Enynes. *ACS Catal.* **2017**, *7*, 1181−1185. (f) Rami, F.; Bächtle, R.; Plietker, B. Hydroboration of internal alkynes catalyzed by FeH(CO)(NO)(PPh3)2: a case of boron-source controlled regioselectivity. *Catal. Sci. Technol.* **2020**, *10*, 1492−1497. (g) Mukherjee, A.; Milstein, D. Homogeneous Catalysis by Cobalt and Manganese Pincer Complexes. *ACS Catal.* **2018**, *8*, 11435−11469.

(6) (a) Obligacion, J. V.; Chirik, P. J. Bis(imino)pyridine Cobalt-Catalyzed Alkene Isomerization-Hydroboration: A Strategy for Remote Hydrofunctionalization with Terminal Selectivity. *J. Am. Chem. Soc.* **2013**, *135*, 19107−19110. (b) Palmer, W. N.; Diao, T.; Pappas, I.; Chirik, P. J. High-Activityl Cobalt Catalysts for Alkene Hydroboration with Electronically Responsive Terpyridine and a-Diimine Ligands. *ACS Catal.* **2015**, *5*, 622−626.

(7) (a) Hayton, T. W.; Legzdins, P.; Sharp, W. B. Coordination and Organometallic Chemistry of Metal-NO Complexes. *Chem. Rev.* **2002**, *102*, 935−992. (b) Ford, P. C.; Lorkovic, I. M. Mechanistic Aspects of the Reactions of Nitric Oxide with Transition-Metal Complexes. *Chem. Rev.* **2002**, *102*, 993−1018. (c) Kaim, W.; Schwederski, B. Non-innocent ligands in bioinorganic chemistry - An overwiev. *Coord. Chem. Rev.* **2010**, *254*, 1580−1588. (d) Jiang, Y.; Schirmer, B.; Blacque, O.; Fox, T.; Grimme, S.; Berke, H. The "Catalytic Nitrosyl Effect": NO Bending Boosting the Efficiency of Rhenium Based Alkene Hydrogenations. *J. Am. Chem. Soc.* **2013**, *135*, 4088−4102.

(8) Pecak, J.; Eder, W.; Stöger, B.; Realista, S.; Martinho, P. N.; Calhorda, M. J.; Linert, W.; Kirchner, K. Synthesis, Characterization, and Catalytic Reactivity of $\{CoNO\}^8$ PCP Pincer Complexes. *Organometallics* **2020**, *39*, 2594−2601.

(9) Krishnan, V. M.; Arman, H. D.; Tonzetich, Z. J. Preparation and reactivity of a square-planar PNP cobalt(II)-hydrido complex: isolation of the first $\{Co\text{-}NO\}^8$-hydride. *Dalton Trans* **2018**, *47*, 1435−1441.

(10) Addison, A. W.; Rao, T. N.; Reedijk, J.; van Rijn, J.; Verschoor, G. C. Synthesis, structure, and spectroscopic properties of copper(II) compounds containing nitrogen-sulphur donor ligands; the crystal and molecular structure of aqua[1,7-bis(N-methylbenzimidazol-2'-yl)-2,6-dithiaheptane]copper(II) perchlorate. *J. Chem. Soc., Dalton Trans.* **1984**, 1349−1356.

(11) Enemark, J. H.; Feltham, R. D. Principles of structure, bonding, and reactivity for metal nitrosyl complexes. *Coord. Chem. Rev.* **1974**, *13*, 339−406.

(12) Selected examples: (a) Haller, K. J.; Enemark, J. H. Structural Chemistry of the $\{CoNO\}^8$ Group. III. The Structure of N,N'-Ethylenebis(salicylideneiminato)nitrosylcobalt(II), Co(NO)(salen). *Acta Crystallogr., Sect. B: Struct. Crystallogr. Cryst. Chem.* **1978**, *B34*, 102−109. (b) Hopmann, K. H.; Conradie, J.; Tangen, E.; Tonzetich, Z. J.; Lippard, S. J.; Ghosh, A. Singlet-Triplet Gaps of Cobalt Nitrosyl: Insight from Tropocoronand Complexes. *Inorg. Chem.* **2015**, *54*, 7362−7367. (c) Pellegrino, J.; Bari, S. E.; Bikiel, D. E.; Doctorovich, F. Successful Stabilization of the Elusive Species $\{FeNO\}^8$ in a Heme Model. *J. Am. Chem. Soc.* **2010**, *132*, 989−995. (d) Enemark, J. H.; Ibers, J. A. The Molecular Structure of Nitrosyldicarbonylbis-(triphenylphosphine)manganese, $Mn(NO)(CO)_2(P(C_6H_5)_3)_2$. *Inorg. Chem.* **1967**, *6*, 1575−1581.

(13) Berke, H.; Burger, P. Nitrosyl Substituted Hydride Complexes-An Activated Class of Compounds. *Comments Inorg. Chem.* **1994**, *16*, 279−312.

(14) Selected examples of metal nitrosyl hydrides: (a) van der Zeijden, A. A. H.; Bürgi, T.; Berke, H. Chromium(0) nitrosyl hydrides. *Inorg. Chim. Acta* **1992**, *201*, 131−135. (b) Liang, F.; Jacobsen, H.; Schmalle, H. W.; Fox, T.; Berke, H. Carbonylhydridonitrosyl(trimethylphosphine)molybdenum(0): An Activated Hydride Complex. *Organometallics* **2000**, *19*, 1950−1962. (c) Dybov, A.; Blacque, O.; Berke, H. Molybdenum and Tungsten Nitrosyl Complexes in Hydrogen Activation. *Eur. J. Inorg. Chem.* **2010**, *2010*, 3328−3337. (d) Choualeb, A.; Maccaroni, E.; Blacque, O.; Schmalle, H. W.; Berke, H. Rhenium Nitrosyl Complexes for Hydrogenation and Hydrosilylations. *Organometallics* **2008**, *27*, 3474−3481. (e) Gusev, D.; Llamazares, A.; Artus, G.; Jacobsen, H.; Berke, H. Classical and Nonclassical Nitrosyl Hydride Complexes of Rhenium in Various Oxidation States. *Organometallics* **1999**, *18*, 75−89. (f) Machura, B. Structural and spectroscopic properties of rhenium nitrosyl complexes. *Coord. Chem. Rev.* **2005**, *249*, 2277−2307. (g) Jänicke, M.; Hund, H. U.; Berke, H. d8-Eisennitrosylhydride. *Chem. Ber.* **1991**, *124*, 719−724.

(15) Murugesan, S.; Stöger, B.; Weil, M.; Veiros, L. F.; Kirchner, K. Synthesis, Structure, and Reactivity of Co(II) and Ni(II) PCP Pincer Borohydride Complexes. *Organometallics* **2015**, *34*, 1364−1372.

(16) (a) Guard, L. M.; Heinekey, D. M. CCDC 1555411: Experimental Crystal Structure Determination, **2017**. DOI: 10.5517/ccdc.csd.cc1p6jkz. (b) Chakraborty, S.; Zhang, J.; Patel, Y. J.; Krause, J. A.; Guan, H. Pincer-Ligated Nickel Hydridoborate Complexes: the Dormant Species in Catalytic Reduction of Carbon Dioxide with Boranes. *Inorg. Chem.* **2013**, *52*, 37−47.

(17) Yunker, L. P.; Stoddard, R. L.; McIndoe, J. S. Practical approaches to the ESI-MS analysis of catalytic reactions. *J. Mass Spectrom.* **2014**, *49*, 1−8.

(18) Perrin, D. D.; Armarego, W. L. F. *Purification of Laboratory Chemicals*, 3rd ed.; Pergamon: New York, 1988.

(19) Bruker computer programs: APEX2, SAINT and SADABS; Bruker AXS Inc.: Madison, WI, 2018.

(20) Sheldrick, G. M. Crystal structure refinement with SHELXL. *Acta Crystallogr., Sect. C: Struct. Chem.* **2015**, *A71*, 3−8.

(21) Sheldrick, G. M. Crystal structure refinement with SHELXL. *Acta Crystallogr., Sect. C: Struct. Chem.* **2015**, *C71*, 3−8.

(22) Macrae, C. F.; Edgington, P. R.; McCabe, P.; Pidcock, E.; Shields, G. P.; Taylor, R.; Towler, M.; van de Streek, J. Mercury: visualization and analysis of crystal structures. *J. Appl. Crystallogr.* **2006**, *39*, 453−457.

(23) Frisch, M. J.; Trucks, G. W.; Schlegel, H. B.; Scuseria, G. E.; Robb, M. A.; Cheeseman, J. R.; Scalmani, G.; Barone, V.; Mennucci, B.; Petersson, G. A.; Nakatsuji, H.; Caricato, M.; Li, X.; Hratchian, H. P.; Izmaylov, A. F.; Bloino, J.; Zheng, G.; Sonnenberg, J. L.; Hada, M.; Ehara, M.; Toyota, K.; Fukuda, R.; Hasegawa, J.; Ishida, M.; Nakajima, T.; Honda, Y.; Kitao, O.; Nakai, H.; Vreven, T.; Montgomery, J. A., Jr.; Peralta, J. E.; Ogliaro, F.; Bearpark, M.; Heyd, J. J.; Brothers, E.; Kudin, K. N.; Staroverov, V. N.; Kobayashi, R.; Normand, J.; Raghavachari, K.; Rendell, A.; Burant, J. C.; Iyengar, S. S.; Tomasi, J.; Cossi, M.; Rega, N.; Millam, J. M.; Klene, M.; Knox,

https://dx.doi.org/10.1021/acs.organomet.0c00755
Organometallics 2021, 40, 278−285

J. E.; Cross, J. B.; Bakken, V.; Adamo, C.; Jaramillo, J.; Gomperts, R.; Stratmann, R. E.; Yazyev, O.; Austin, A. J.; Cammi, R.; Pomelli, C.; Ochterski, J. W.; Martin, R. L.; Morokuma, K.; Zakrzewski, V. G.; Voth, G. A.; Salvador, P.; Dannenberg, J. J.; Dapprich, S.; Daniels, A. D.; Farkas, Ö.; Foresman, J. B.; Ortiz, J. V.; Cioslowski, J.; Fox, D. J. *Gaussian 09*, revision A.02; Gaussian, Inc.: Wallingford, CT, 2009.

(24) Hehre, W. J.; Radom, L.; Schleyer, P. v. R.; Pople, J. A. *Ab Initio Molecular Orbital Theory*; John Wiley & Sons: New York, 1986.

(25) Parr, R. G.; Yang, W. *Density Functional Theory of Atoms and Molecules*; Oxford University Press: New York, 1989.

(26) (a) Perdew, J. P.; Burke, K.; Ernzerhof, M. Generalized Gradient Approximation Made Simple. *Phys. Rev. Lett.* **1996**, *77*, 3865−3868. (b) Perdew, J. P.; Burke, K.; Ernzerhof, M. Generalized Gradient Approximation Made Simple. *Phys. Rev. Lett.* **1997**, *78*, 1396−1396. (c) Perdew, J. P. Density-functional approximation for the correlation energy of the inhomogeneous electron gas. *Phys. Rev. B: Condens. Matter Mater. Phys.* **1986**, *33*, 8822−8824.

(27) (a) Haussermann, U.; Dolg, M.; Stoll, H.; Preuss, H.; Schwerdtfeger, P.; Pitzer, R.M. Accuracy of energy-adjusted quasirelativistic ab initio pseudopotentials. *Mol. Phys.* **1993**, *78*, 1211−1224. (b) Kuechle, W.; Dolg, M.; Stoll, H.; Preuss, H. Energy-adjusted pseudopotentials for the actinides. Parameter sets and test calculations for thorium and thorium monoxide. *J. Chem. Phys.* **1994**, *100*, 7535−7542. (c) Leininger, T.; Nicklass, A.; Stoll, H.; Dolg, M.; Schwerdtfeger, P. The accuracy of the pseudopotential approximation. II. A comparison of various core sizes for indium pseudopotentials in calculations for spectroscopic constants of InH, InF, and InCl. *J. Chem. Phys.* **1996**, *105*, 1052−1059.

(28) (a) Ditchfield, R.; Hehre, W. J.; Pople, J. A. Self-Consistent Molecular-Orbital Methods. IX. An Extended Gaussian-Type Basis for Molecular-Orbital Studies of Organic Molecules. *J. Chem. Phys.* **1971**, *54*, 724−728. (b) Hehre, W. J.; Ditchfield, R.; Pople, J. A. Self-Consistent Molecular Orbital Methods. 12. Further extensions of Gaussian-type basis sets for use in molecular-orbital studies of organic-molecules. *J. Chem. Phys.* **1972**, *56*, 2257−2261. (c) Hariharan, P. C.; Pople, J. A. Accuracy of AH equilibrium geometries by single determinant molecular-orbital theory. *Mol. Phys.* **1974**, *27*, 209−214. (d) Gordon, M. S. The isomers of silacyclopropane. *Chem. Phys. Lett.* **1980**, *76*, 163−168. (e) Hariharan, P. C.; Pople, J. A. Influence of polarization functions on molecular-orbital hydrogenation energies. *Theor. Chim. Acta* **1973**, *28*, 213−222.

(29) (a) Peng, C.; Ayala, P. Y.; Schlegel, H. B.; Frisch, M. J. Using redundant internal coordinates to optimize equilibrium geometries and transition states. *J. Comput. Chem.* **1996**, *17*, 49−56. (b) Peng, C.; Schlegel, H. B. Combining Synchronous Transit and Quasi-Newton Methods for Finding Transition States. *Isr. J. Chem.* **1993**, *33*, 449−454.

(30) Grimme, S.; Antony, J.; Ehrlich, S.; Krieg, H. A consistent and accurate ab initio parameterization of density functional dispersion correction (DFT-D) for the 94 elements H-Pu. *J. Chem. Phys.* **2010**, *132*, 154104.

(31) (a) Becke, A. D.; Johnson, E. R. A density-functional model of the dispersion interaction. *J. Chem. Phys.* **2005**, *123*, 154101. (b) Johnson, E. R.; Becke, A. D. A post-Hartree-Fock model of intermolecular interactions. *J. Chem. Phys.* **2005**, *123*, 024101. (c) Johnson, E. R.; Becke, A. D. A post-Hartree-Fock model of intermolecular interactions: Inclusion of higher-order corrections. *J. Chem. Phys.* **2006**, *124*, 174104.

(32) (a) Carpenter, J. E.; Weinhold, F. Analysis of the geometry of the hydroxymethyl radical by the "different hybrids for different spins" natural bond orbital procedure. *J. Mol. Struct.: THEOCHEM* **1988**, *169*, 41−62. (b) Carpenter, J. E. Extension of Lewis structure concepts to open-shell and excited-state molecular species. Ph.D. Thesis. University of Wisconsin, Madison, WI, 1987. (c) Foster, J. P.; Weinhold, F. Natural hybrid orbitals. *J. Am. Chem. Soc.* **1980**, *102*, 7211−7218. (d) Reed, A. E.; Weinhold, F. Natural bond orbital analysis of near-Hartree-Fock water dimer. *J. Chem. Phys.* **1983**, *78*, 4066−4073. (e) Reed, A. E.; Weinhold, F. Natural localized molecular orbitals. *J. Chem. Phys.* **1985**, *83*, 1736−1740. (f) Reed, A. E.; Weinstock, R. B.; Weinhold, F. Natural population analysis. *J. Chem. Phys.* **1985**, *83*, 735−746. (g) Reed, A. E.; Curtiss, L. A.; Weinhold, F. Intermolecular interactions from a natural bond orbital, donor-acceptor viewpoint. *Chem. Rev.* **1988**, *88*, 899−926. (h) Weinhold, F.; Carpenter, J. E. *The Structure of Small Molecules and Ions*; Plenum: New York, 1988; p 227.

(33) Glendening, E. D.; Badenhoop, J. K.; Reed, A. E.; Carpenter, J. E.; Bohmann, J. A.; Morales, C. M.; Weinhold, F. *NBO 5.0*; Theoretical Chemistry Institute, University of Wisconsin: Madison, WI, 2001.

(34) Portmann, S.; Lüthi, H. P. MOLEKEL: An Interactive Molecular Graphics Tool. *Chimia* **2000**, *54*, 766−770.

https://dx.doi.org/10.1021/acs.organomet.0c00755
Organometallics 2021, 40, 278−285